

Developing a tetO/TetR system in Neurospora crassa

Tinh-Suong Nguyen, Eugene Gladyshev

▶ **To cite this version:**

Tinh-Suong Nguyen, Eugene Gladyshev. Developing a tetO/TetR system in Neurospora crassa. Fungal Genetics and Biology, 2020, 136, pp.103316. 10.1016/j.fgb.2019.103316 . pasteur-03261456

HAL Id: pasteur-03261456
https://pasteur.hal.science/pasteur-03261456

Submitted on 21 Jul 2022

HAL is a multi-disciplinary open access archive for the deposit and dissemination of scientific research documents, whether they are published or not. The documents may come from teaching and research institutions in France or abroad, or from public or private research centers.

L'archive ouverte pluridisciplinaire **HAL**, est destinée au dépôt et à la diffusion de documents scientifiques de niveau recherche, publiés ou non, émanant des établissements d'enseignement et de recherche français ou étrangers, des laboratoires publics ou privés.



Distributed under a Creative Commons Attribution - NonCommercial 4.0 International License

Version of Record: https://www.sciencedirect.com/science/article/pii/S1087184519303615
Manuscript_7927af708021ba3f90170263c92dc73b

TITLE

Developing a *tetO*/TetR system in *Neurospora crassa*

AUTHORS

Tinh-Suong Nguyen & Eugene Gladyshev*

AFFILIATION

Group Fungal Epigenomics, Department of Mycology, Institut Pasteur, Paris 75015, France

*Corresponding address: eugene.gladyshev@gmail.com

TYPE

Resource

ABSTRACT

The development of a *tetO*/TetR system in the fungus *Neurospora crassa* is described. The system includes (i) a synthetic gene encoding a TetR variant fused to GFP, and (ii) a standard *tetO* array integrated homologously, as a proof of principle, near the *his-3* gene. The localization of TetR-GFP at the *tetO* array (observed by fluorescence microscopy) can be disrupted by the application of tetracycline. The full-length array is stable during vegetative growth, but it triggers strong repeat-induced point mutation (RIP) by the RID-dependent as well as the DIM-2-dependent pathways during the sexual phase. Thus, both RIP pathways must be inactivated to allow the faithful inheritance of the unmodified construct. In summary, this study introduces a new molecular tool into Neurospora research, and suggests that the standard *tetO* array can self-engage in recombination-independent homologous pairing.

KEYWORDS

Fluorescent repressor operator system; FROS; TetR; tetO; Repeat-induced point mutation; RIP; Neurospora

INTRODUCTION

The high yet controllable affinity of the tetracycline repressor TetR for the *tetO* operator sequence has been used widely to visualize and manipulate chromosomal loci in diverse organisms (Berens and Hillen, 2004). One such approach involves labeling *tetO*-containing loci with TetR fused to a fluorescent protein, *e.g.*, GFP (Fluorescent repressor operator system, FROS). Normally, several to many dozens of *tetO* sites must be present at a given locus (in the form of an array) to ensure their detection by conventional fluorescence microscopy (Michaelis et

© 2019 published by Elsevier. This manuscript is made available under the CC BY NC user license
https://creativecommons.org/licenses/by-nc/4.0/

al., 1997). One commonly used *tetO* array was engineered by Lau, Sherratt and colleagues (2003). This construct contains approximately 240 individual *tetO* sites interspersed with short runs of random sequences over the total length of ~9 kb (Lau et al., 2003). The presence of random sequences between *tetO* sites was necessary to reduce the instability of the array due to its otherwise highly repetitive nature.

The model fungus *Neurospora crassa* features a potent genome-defense process, known as repeat-induced point mutation (RIP), which occurs in haploid nuclei that divide by mitosis in preparation for karyogamy and ensuing meiosis (Selker, 1990; Gladyshev, 2017). RIP possesses a remarkable ability to recognize and mutate (by C-to-T transitions) nearly all gene-sized DNA repeats. Duplications are detected irrespective of their specific nucleotide composition, origin, and genomic positions (Selker, 1990; Gladyshev, 2017). We have previously shown that RIP involves a mechanism of sequence homology recognition that cross-matches segments of chromosomal DNA as arrays of interspersed base-pair triplets (Gladyshev and Kleckner, 2014). This process can be very efficient yet it does not require the RecA/Rad51/Dmc1 proteins (Gladyshev and Kleckner, 2014). We have also found that RIP can be mediated by an epigenetic pathway that includes a conserved SUV39 lysine methyltransferase DIM-5 (which catalyzes trimethylation of histone H3 lysine-9) and a DNMT1-like cytosine methyltransferase DIM-2, which is recruited to H3K9me3-containing loci by its direct interaction with HP1 (Aramayo and Selker, 2013). This heterochromatin-related pathway appears largely independent from the canonical RIP pathway mediated by a putative cytosine methyltransferase RID ("RIP defective", Freitag et al., 2002).

This study reports the development and validation of the *tetO*/TetR system in *N. crassa*. The system includes a standard full-length *tetO* array (Lau et al., 2003) and a codon-optimized gene encoding a chimeric TetR variant fused to GFP. The stability of the array has been examined in both vegetative and sexual phases. The capacity of the TetR-GFP/tetO interaction to be controlled by the application of tetracycline has also been evaluated.

RESULTS

The full-length *tetO* array can be integrated into the *N. crassa* genome by homologous recombination

The array-containing *Xba*I-*Nhe*I fragment of pLAU44 (Lau et al., 2003) was inserted into pMF272 (Freitag et al., 2004) to produce pTSN6 (Fig. 1A; GenBank acc. MN249407). Plasmid pTSN6 was linearized with *Nde*I and transformed into a standard *his-3* strain FGSC#9270 (Colot et al., 2006). Primary *his-3*+ transformants were first screened by PCR to select those carrying the intact array (Fig. 1A; Methods). One homokaryotic transformant (strain "A", purified by macroconidiation) was selected for further analysis (Fig. 1C,D).

The full-length *tetO* array is stable during vegetative growth in *N. crassa*

The overall stability of the array during vegetative growth was assayed by a protocol that included the following steps: first, strain "A" was allowed to grow and produce macroconidia; second, a large number of macroconidia

was transferred onto iodoacetate agar to induce microconidiation (i.e., the production of spores with only one nucleus); third, microconidia were purified by filtration and germinated; fourth, microconidial isolates were analyzed by PCR for the presence of the *GmR* (*gentamicin-resistant*) marker (Fig. 1E). The failure to obtain the expected PCR product would have indicated a loss (or rearrangement) of the *GmR* sequence at any moment before the germination of microconidia. The choice of *GmR* as the tester region was influenced by the fact that enforcing its retention in *E. coli* was sufficient to ensure the integrity of the entire construct (Lau et al., 2003). No loss of *GmR* was observed in a random sample of 30 microconidial isolates, suggesting that the full-length array remained reasonably stable in vegetative nuclei (Fig. 1E: left panel).

Full-length *tetO* array triggers strong repeat-induced point mutation (RIP)

The ability of RIP to detect interspersed homology sets it aside from recombination-mediated mechanisms that require high levels of overall sequence similarity. Therefore, it was possible that a large number of short *tetO* sequences could potentially comprise an instance of interspersed homology that could trigger RIP. To test this possibility, strain "A" was crossed to another *rid*+ strain of the opposite mating type (FGSC#9539, McCluskey et al., 2010) and the occurrence of RIP in the two separate regions was analyzed by sequencing (Methods). Very strong RIP was observed within the repetitive portion of the construct, with the frequency of mutation reaching 90-100% at many sites (Fig. 1G: "Wildtype").

In *N. crassa*, RIP can occur in the absence of RID, in which case it requires a set of factors normally involved in the assembly of constitutive heterochromatin, including DIM-5, a lysine methyltransferase, and DIM-2, a C5-cytosine methyltransferase (Aramayo and Selker, 2013; Gladyshev and Kleckner, 2017). To investigate the specific contribution of the DIM-5/DIM-2-dependent RIP in mutation of the *tetO* array, the latter was integrated into the *his-3* locus of a previously published *ridΔ* strain C146.1 (Gladyshev and Kleckner, 2017). The resulting strain "B" (Fig. 1C) also contained the following gene deletions: *dim-5Δ*, *set-7Δ* and *mus-52Δ* (Fig. 1D). While *set-7Δ* does not impede RIP in *N. crassa* (Gladyshev and Kleckner, 2017), it is required for the restoration of fertility of *dim-5Δ* strains (Jamieson et al., 2013). Strain "B" was crossed to a previously published *ridΔ* strain C02.1 (Gladyshev and Kleckner, 2017). Both parents were wildtype with respect to *dim-2*+. Thus, while the RID-dependent RIP was completely inactivated, the DIM-5/DIM-2-dependent RIP was only partially attenuated in the *dim-5Δ/*+ background (Fig. 1G: "RID-deficient"). Substantial levels of RIP could still be observed, with individual mutations being distributed rather uniformly across the analyzed regions (Fig. 1G: "RID-deficient"). Importantly, C-to-T and G-to-A mutations were the only types of changes in the DNA sequence detected within the analyzed regions in the progeny of both crosses (N=48). In particular, no deletions (even of a single base-pair) have been observed.

Recently, we have developed a new numerical approach to analyzing distributions of individual RIP mutations

called partitioned RIP propensity (PRP). The algorithm considers only mutation of CpA (or TpG) dinucleotides (the preferred substrate of RIP in *N. crassa*) and effectively treats small overlapping DNA segments (rather than individual sites) as units of mutation (Mazur and Gladyshev, 2018). Previously, we used this method to analyze pairs of closely-positioned repeats, where each construct corresponded to only one specific paired conformation (Mazur and Gladyshev, 2018). In contrast, the presence of many identical *tetO* sites distributed over the 9-kp region permits a much larger number of alternative pairing configurations. This situation would be reminiscent of any natural genomic region containing many repeat units (such as satellite DNA). In such a case, the observed PRP profiles would represent the average (expected) outcome of many pairing conformations. For the *tetO* array, we find that the fine structure of the PRP profile of the DIM-5/DIM-2-dependent RIP is similar to the wildtype case, in which the RID-dependent pathway strongly predominates (Fig. 1G,H). This result hints at a possibility that the two pathways of mutation may share a common step.

Design and expression of the codon-optimized *tetR-gfp* gene

Having evaluated basic properties of the *tetO* array in *N. crassa*, we proceed to expressing its cognate binding partner, the TetR repressor. Our initial attempts to produce a common TetR-GFP variant (Lau et al., 2003) in *N. crassa* using a "standard" *ccg-1* promoter (Freitag et al., 2004) were unsuccessful (data not shown). Thus, we decided to engineer a synthetic *tetR-gfp* gene by following a previously published approach (Gooch et al., 2008). To this end, we used an amino-acid sequence of a chimeric TetR variant lacking all cysteine residues (Luckner et al., 2007). We chose this variant because it was more stable and less prone to aggregation (Luckner et al., 2007). A nuclear localization signal PRRKKRK was inserted into a short linker region separating TetR and GFP (Fig. 1B). The sequence encoding TetR-NLS-GFP was placed under the control of the constitutive *trpC* promoter subcloned from pCSN44 (Staben et al., 1989). The construct was inserted into a derivative of pMF272 (Freitag et al., 2004) to produce pTSN7A (GenBank acc. MN249408). In parallel, the same construct was also inserted into a derivative of pCSR1 (Bardiya and Shiu, 2007) to produce pTSN7B (GenBank acc. MN249409), which was used to integrate *tetR-gfp* as the replacement of the *csr-1* gene (below).

To investigate if (1) TetR-NLS-GFP could be produced in *N. crassa* in principle and (2) its localization at the *tetO* array could be observed by fluorescence microscopy, pTSN7B (linearized with *Ahd*I) was transformed into strain "A" to produce strain "C" (Fig. 1C,D). In vegetative cells of strain "C", one bright GFP spot per nucleus could be detected (Fig. 1F). In addition, substantial diffuse nuclear GFP signal was also observed. This signal likely corresponds to the excess of TetR-NLS-GFP, as it was absent in the wildtype strain FGSC#4200 (Fig. 1F). To verify that the presence of the GFP spot required the array, the *tetO::his-3+* and *tetR-gfp::csr-1Δ* loci were separated by crossing strain "C" to FGSC#4200 (Fig. 1C). From this cross, a new strain was isolated that carried *tetR-gfp::csr-1Δ* but not *tetO::his-3+* (strain "D"; Fig. 1C,D). In this strain, the diffuse nuclear signal could still be observed, but not the GFP spot, suggesting that the latter indeed corresponded to TetR-NLS-GFP localized at

the array (Fig. 1F: Strain "D"). Importantly, the array itself remained stable in the presence of TetR-NLS-GFP (Fig. 1E, right panel).

The association of TetR-NLS-GFP with the tetO array is controllable

One advantage of the *tetO*/TetR system over the other tethering approaches (*e.g.*, Gessaman and Selker, 2017) is its capacity to be regulated by the addition of tetracycline. To investigate if the localization of TetR-NLS-GFP at the *tetO* array could be disrupted pharmacologically, mycelial cultures of strain "C" were supplemented with tetracycline at the final concentration of 5 μg/ml, grown for 30 min, and imaged by fluorescence microscopy. As shown in Fig. 1F, the addition of tetracycline has resulted in the disappearance of the GFP spot, suggesting that the *tetO*/TetR interaction can indeed be controlled pharmacologically in *N. crassa.*

DISCUSSION

Our study has yielded two principal results. First, it introduces the *tetO*/TetR system into *N. crassa*. Specifically, it shows that the *tetO*/TetR interaction provides a reliable basis for FROS while also being readily controlled by tetracycline. These features should enable previously unattainable experimental approaches, such as imaging the dynamics of chromatin and chromosomes (including homologous pairing) or manipulating the association of various proteins with *tetO*-containing loci (*e.g.*, Ragunathan et al., 2015).

Second, our study demonstrates an intrinsic ability of the standard *tetO* array to trigger strong RIP by the RID-dependent as well as the DIM-5/DIM-2-dependent pathways. This finding suggests that the array may produce a *de novo* signal for nucleating heterochromatin. Previously, studies in *Saccharomyces cerevisiae* have described the formation of heterochromatin at this construct, but only in the presence of the tightly bound TetR molecules (Dubarry et al., 2011). In contrast, RIP is triggered in the absence of TetR in this study. Given the proposed mechanism of homology recognition for RIP (Gladyshev and Kleckner, 2014), this result advances a possibility that the widely used construct, due to its highly repetitive nature, may be able to self-engage in recombination-independent homologous pairing. This property may become useful in understanding the mechanism of RIP as it affords a powerful molecular system to generate putative homologous dsDNA-dsDNA interactions as well as to modulate them by recruiting candidate effector proteins.

METHODS

Manipulation of Neurospora strains

FGSC#4200, FGSC#9539 and FGSC#9720 were obtained from the Fungal Genetics Stock Center (McCluskey et al., 2010). Strains C02.1 and C146.1 were published previously (Gladyshev and Kleckner, 2017). Vegetative

cultures were grown at 30ºC in Vogel's medium (Vogel, 1956) containing 1.5% sucrose. Crosses were setup on Synthetic Crossing medium (Westergaard and Mitchell, 1947), solidified with 2% agar and supplemented with 2% sucrose. Microconidia were obtained by the protocol of Ebbole and Sachs (1990). All types of spores were plated on sorbose agar (2% sorbose, 0.1% dextrose, 1x Vogel's medium, 3% agar) to induce colonial growth.

Plasmids

To make pTSN6, *Xba*I-*Nhe*I fragment of pLAU44 (Lau et al., 2003) was purified by agarose gel electrophoresis and inserted into a derivative of pFM272 (Freitag et al., 2004), in which the sequence between *Not*I and *Eco*RI sites was replaced with C<u>TCTAGA</u>C (*Xba*I site underlined). The entire subcloned segment was sequenced by primer walking. The synthetic sequence encoding the chimeric TetR variant (Luckner et al., 2007) was ordered as a "gBlock" from Integrated DNA Technologies (IDT). DNA of plasmids pTSN6, pTSN7A and pTSN7B has been deposited at AddGene (Watertown, MA, USA).

Transformation

Linearized plasmids pTSN6 and pTSN7B were transformed into macroconidia by electroporation as previously described (Gladyshev and Kleckner, 2014). Both recipient strains (FGSC#9720 and C146.1) carried the deletion of *mus-52* (normally encoding KU80, an essential component of the nonhomologous end-joining system), which was necessary to avoid ectopic insertion events (Ninomiya et al., 2004). If necessary, homokaryotic strains were purified from primary heterokaryotic transformants by macroconidiation.

Genotyping

Genomic DNA was extracted exactly as previously described (Gladyshev and Kleckner, 2014).

Gene deletions

For each isolate, PCR master mix was prepared containing reaction buffer, nucleotides, Taq polymerase (Thermo Scientific, cat. no. EP0402) and genomic DNA but not the primers. Each strain-specific master mix was split into 8 PCR tubes, and one gene-specific primer pair was then added to each tube. The following primers were used: DIM2_F/DIM2_R (*dim-2*), DIM5_F/DIM5_R (*dim-5*), HIS3_F/HIS3_R (*his-3*), MATA_F/MATA_R (*mat A*), MUS52_F/MUS52_R (*mus-52*), RID_F/RID_R (*rid*), CSR1_F/CSR1_R (*csr-1*). Primer sequences are provided in Supplementary Table 1. PCRs were run on the same block and the products were resolved on 1% agarose gels.

The full-length tetO array

Two overlapping halves of the array were amplified using the Expand Long Template PCR System (Sigma, cat. no. 11681834001) with the following primers: LF/LR ("left" half") and RF/RR ("right" half) (Supplementary Table 1). Diluted pTSN6 was used as a positive control.

GmR marker

Microconidial isolates was genotyped using Taq polymerase (Thermo Scientific, cat. no. EP0402) and the primer combination RF/LR (Supplementary Table 1).

Microscopy

Vegetative cultures were started from frozen macroconidia and allowed to grow for 12 hours. When required, the cultures were supplemented with tetracycline (Sigma, cat. no. T7660) at the final concentration of 5 μg/ml. Live mycelia were spread on glass slides and imaged on a Zeiss upright microscope using a 100x objective.

Analysis of RIP mutations

A random sample of 24 "late" progeny spores was analyzed for each condition (corresponding to a single cross). The "left" arm of the *tetO* array was amplified by PCR using Phusion High-Fidelity DNA Polymerase (NEB, cat. no. M0530L) and the primers LF/LR (Supplementary Table 1). PCR products were purified using the E.Z.N.A. Cycle Pure Kit (Omega Bio-tek) and sequenced directly by primer walking. Chromatograms were assembled into contigs using Phred/Phrap (Ewing et al., 1998). All assemblies were validated manually using Consed (Gordon et al., 1998). For each cross, contigs were aligned to the reference sequence using ClustalW (Thompson et al., 1994). Sequence alignments (in the ClustalW format) are provided as Supplementary Data. RIP mutations were analyzed as previously described (Gladyshev and Kleckner, 2014; Mazur and Gladyshev, 2018).

ACKNOWLEDGMENTS

The work was supported by grants from the Agence Nationale de la Recherche (10-LABX-0062) and Fondation pour la Recherche Médicale (AJE20180539525).

FIGURE LEGENDS

Figure 1. Developing a *tetO*/TetR system in *N. crassa*

(A) Plasmid pTSN6 (GenBank acc. MN249407) carries the full-length *tetO* array subcloned from pLAU44 (Lau et al., 2003). The array contains approximately 240 *tetO* sites and is interrupted in the middle by the *GmR* gene, which confers resistance to gentamicin (Lau et al., 2003). Primer pairs LF/LR and RF/RR are used to amplify the "left" and the "right" halves of the array, respectively. Two regions within the "left" half of the array (horizontal red bars) are analyzed for RIP mutation in G,H.

(B) Plasmid pTSN7B (GenBank acc. MN249409) is used to integrate *tetR-gfp* as the replacement of the *csr-1+*. gene. Nuclear localization sequence (NLS) is underlined. The constitutive *trpC* promoter (Staben et al., 1989)

was used for expression.

(C) Strains “A” and “C” are derived from FGSC#9720 (Colot et al., 2006) by homologous transformation. Strain “D” is the F1 progeny of the cross between strain “C” and FGSC#4200 (McCluskey et al., 2010). Strain “B” is derived from C146.1 (Gladyshev and Kleckner, 2017) by homologous transformation.

(D) Strains are genotyped for the presence of the indicated wildtype alleles (Methods). *GmR* was amplified using primers RF/LR, shown in A. *his-3** is an intergenic region replaced by the *tetO* array.

(E) The stability of the *tetO* array during vegetative growth is evaluated by quantifying the retention of the *GmR* marker in random microconidial isolates.

(F) Observing the expression and localization of TetR-NLS-GFP by fluorescence microscopy. Mycelial cultures were started from resting macroconidia and grown for 12 hours. Mycelia were spread on glass slides and imaged on a Zeiss upright microscope using a 100x objective. Tetracycline was added to the final concentration of 5 μg/ml.

(G) RIP mutation of the full-length *tetO* array. A random sample of 24 “late” spores was analyzed for each condition. In the “Wildtype” condition, both RIP pathways were active. In the “RID-deficient” condition, the RID-dependent pathway was inactivated, while the DIM-5/DIM-2-dependent pathway was partially attenuated. Genotypes of parental strains (P1 and P2) are indicated. Aligned sequences are provided as Supplementary Data.

(H) Partitioned RIP propensity (PRP) profiles constructed for data in H. Profiles are shifted along the y-axis to facilitate their visual comparison.

REFERENCES

Aramayo, R., Selker, E.U., 2013. *Neurospora crassa*, a model system for epigenetics research. Cold Spring Harb Perspect Biol 5, a017921. https://doi.org/10.1101/cshperspect.a017921

Bardiya, N., Shiu, P.K.T., 2007. Cyclosporin A-resistance based gene placement system for *Neurospora crassa*. Fungal Genet. Biol. 44, 307–314. https://doi.org/10.1016/j.fgb.2006.12.011

Berens, C., Hillen, W., 2004. Gene regulation by tetracyclines. Genet. Eng. (N.Y.) 26, 255–277.

Colot, H.V., Park, G., Turner, G.E., Ringelberg, C., Crew, C.M., Litvinkova, L., Weiss, R.L., Borkovich, K.A., Dunlap, J.C., 2006. A high-throughput gene knockout procedure for Neurospora reveals functions for multiple transcription factors. Proc. Natl. Acad. Sci. U.S.A. 103, 10352–10357.

https://doi.org/10.1073/pnas.0601456103

Dubarry, M., Loïodice, I., Chen, C.L., Thermes, C., Taddei, A., 2011. Tight protein-DNA interactions favor gene silencing. Genes Dev. 25, 1365–1370. https://doi.org/10.1101/gad.611011

Ebbole, D., Sachs, M.S., 1990. A rapid and simple method for isolation of *Neurospora crassa* homokaryons using microconidia. Fungal Genetics Reports 37. https://doi.org/10.4148/1941-4765.1472

Ewing, B., Hillier, L., Wendl, M.C., Green, P., 1998. Base-Calling of Automated Sequencer Traces Using *Phred.* I. Accuracy Assessment. Genome Res. 8, 175–185. https://doi.org/10.1101/gr.8.3.175

Freitag, M., Hickey, P.C., Raju, N.B., Selker, E.U., Read, N.D., 2004. GFP as a tool to analyze the organization, dynamics and function of nuclei and microtubules in *Neurospora crassa*. Fungal Genet. Biol. 41, 897–910. https://doi.org/10.1016/j.fgb.2004.06.008

Freitag, M., Williams, R.L., Kothe, G.O., Selker, E.U., 2002. A cytosine methyltransferase homologue is essential for repeat-induced point mutation in *Neurospora crassa*. Proc. Natl. Acad. Sci. U.S.A. 99, 8802–8807. https://doi.org/10.1073/pnas.132212899

Gessaman, J.D., Selker, E.U., 2017. Induction of H3K9me3 and DNA methylation by tethered heterochromatin factors in *Neurospora crassa*. Proc Natl Acad Sci USA 114, E9598–E9607. https://doi.org/10.1073/pnas.1715049114

Gladyshev, E., 2017. Repeat-Induced Point Mutation and Other Genome Defense Mechanisms in Fungi. Microbiol Spectr 5. https://doi.org/10.1128/microbiolspec.FUNK-0042-2017

Gladyshev, E., Kleckner, N., 2017. DNA sequence homology induces cytosine-to-thymine mutation by a heterochromatin-related pathway in Neurospora. Nat. Genet. 49, 887–894. https://doi.org/10.1038/ng.3857

Gladyshev, E., Kleckner, N., 2014. Direct recognition of homology between double helices of DNA in *Neurospora crassa*. Nat Commun 5, 3509. https://doi.org/10.1038/ncomms4509

Gordon, D., Abajian, C., Green, P., 1998. *Consed:* A Graphical Tool for Sequence Finishing. Genome Res. 8, 195–202. https://doi.org/10.1101/gr.8.3.195

Gooch, V.D., Mehra, A., Larrondo, L.F., Fox, J., Touroutoutoudis, M., Loros, J.J., Dunlap, J.C., 2008. Fully codon-optimized luciferase uncovers novel temperature characteristics of the Neurospora clock. Eukaryotic Cell 7, 28–37. https://doi.org/10.1128/EC.00257-07

Jamieson, K., Rountree, M.R., Lewis, Z.A., Stajich, J.E., Selker, E.U., 2013. Regional control of histone H3 lysine 27 methylation in Neurospora. Proc. Natl. Acad. Sci. U.S.A. 110, 6027–6032. https://doi.org/10.1073/pnas.1303750110

Lau, I.F., Filipe, S.R., Søballe, B., Økstad, O.-A., Barre, F.-X., Sherratt, D.J., 2003. Spatial and temporal organization of replicating Escherichia coli chromosomes. Mol. Microbiol. 49, 731–743.

Luckner, S.R., Klotzsche, M., Berens, C., Hillen, W., Muller, Y.A., 2007. How an agonist peptide mimics the antibiotic tetracycline to induce Tet-repressor. J. Mol. Biol. 368, 780–790.

https://doi.org/10.1016/j.jmb.2007.02.030

Mazur, A.K., Gladyshev, E., 2018. Partition of Repeat-Induced Point Mutations Reveals Structural Aspects of Homologous DNA-DNA Pairing. Biophys. J. 115, 605–615. https://doi.org/10.1016/j.bpj.2018.06.030

McCluskey, K., Wiest, A., Plamann, M., 2010. The Fungal Genetics Stock Center: a repository for 50 years of fungal genetics research. J. Biosci. 35, 119–126.

Michaelis, C., Ciosk, R., Nasmyth, K., 1997. Cohesins: chromosomal proteins that prevent premature separation of sister chromatids. Cell 91, 35–45.

Ninomiya, Y., Suzuki, K., Ishii, C., Inoue, H., 2004. From The Cover: Highly efficient gene replacements in Neurospora strains deficient for nonhomologous end-joining. Proceedings of the National Academy of Sciences 101, 12248–12253. https://doi.org/10.1073/pnas.0402780101

Ragunathan, K., Jih, G., Moazed, D., 2015. Epigenetic inheritance uncoupled from sequence-specific recruitment. Science 348, 1258699. https://doi.org/10.1126/science.1258699

Selker, E.U., 1990. Premeiotic instability of repeated sequences in *Neurospora crassa*. Annu. Rev. Genet. 24, 579–613. https://doi.org/10.1146/annurev.ge.24.120190.003051

Staben, C., Jensen, B., Singer, M., Pollock, J., Schechtman, M., Kinsey, J., Selker, E., 1989. Use of a bacterial hygromycin B resistance gene as a dominant selectable marker in *Neurospora crassa* transformation. Fungal Genetics Reports 36, 79. https://doi.org/10.4148/1941-4765.1519

Thompson, J.D., Higgins, D.G., Gibson, T.J., 1994. CLUSTAL W: improving the sensitivity of progressive multiple sequence alignment through sequence weighting, position-specific gap penalties and weight matrix choice. Nucl Acids Res 22, 4673–4680. https://doi.org/10.1093/nar/22.22.4673

Vogel, H.J. 1956. A Convenient Growth Medium for *Neurospora crassa*. Microbial Genetics Bulletin 13, 42-47.

Westergaard, M., Mitchell, H.K., 1947. Neurospora V. A synthetic medium favoring sexual reproduction. American Journal of Botany 34, 573–577. https://doi.org/10.1002/j.1537-2197.1947.tb13032.x

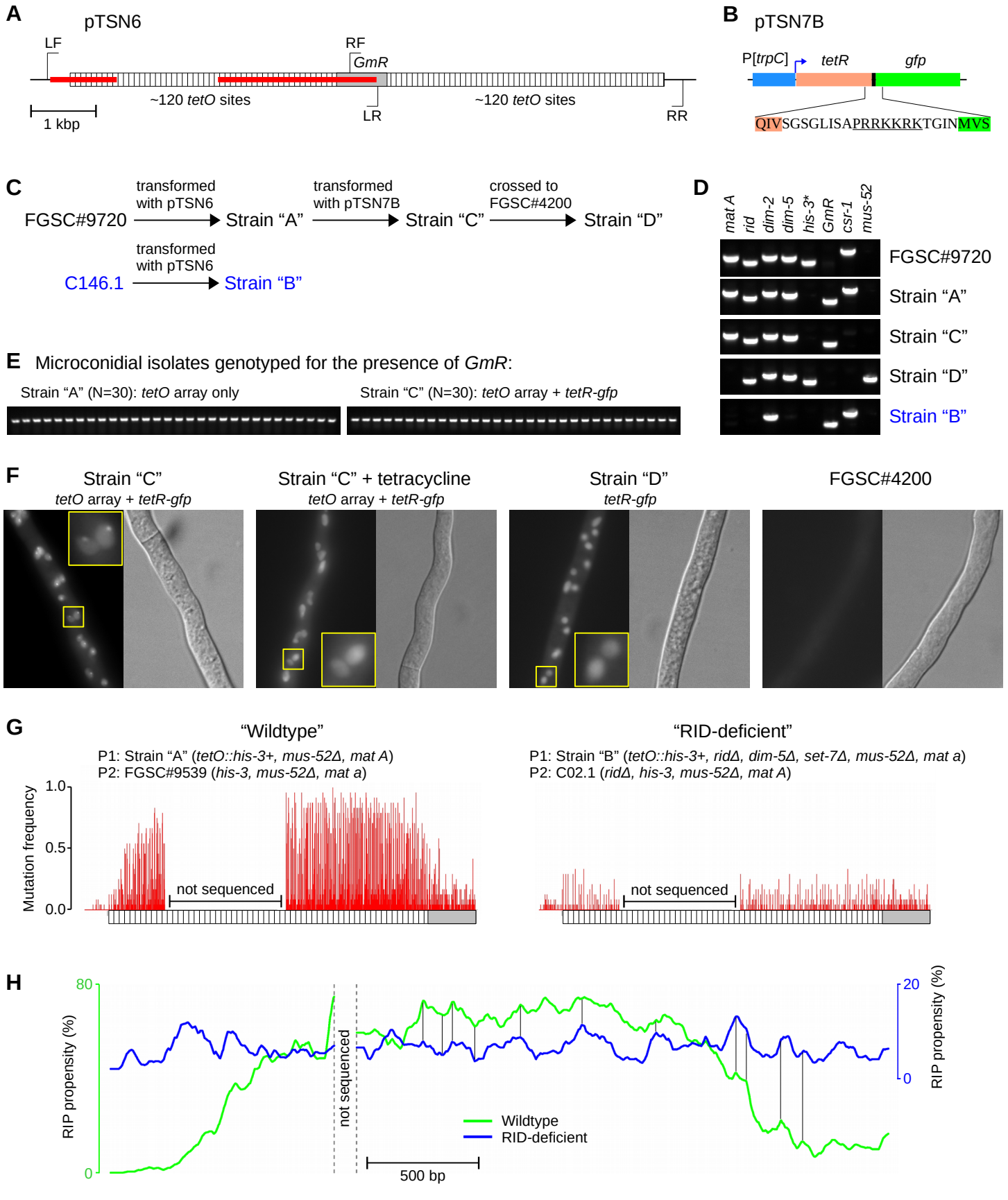

A
pTSN6
LF
RF
GmR
~120 tetO sites
~120 tetO sites
1 kbp
LR
RR
B
pTSN7B
P[trpC]
tetR
gfp
QIVSGSGLISAPRRKKRKTGINMVS
C
FGSC#9720
transformed with pTSN6
Strain "A"
transformed with pTSN7B
Strain "C"
crossed to FGSC#4200
Strain "D"
C146.1
transformed with pTSN6
Strain "B"
D
mat A
rid
dim-2
dim-5
his-3*
GmR
csr-1
mus-52
FGSC#9720
Strain "A"
Strain "C"
Strain "D"
Strain "B"
E
Microconidial isolates genotyped for the presence of GmR:
Strain "A" (N=30): tetO array only
Strain "C" (N=30): tetO array + tetR-gfp
F
Strain "C"
tetO array + tetR-gfp
Strain "C" + tetracycline
tetO array + tetR-gfp
Strain "D"
tetR-gfp
FGSC#4200
G
"Wildtype"
P1: Strain "A" (tetO::his-3+, mus-52Δ, mat A)
P2: FGSC#9539 (his-3, mus-52Δ, mat a)
Mutation frequency
1.0
0.5
0.0
not sequenced
"RID-deficient"
P1: Strain "B" (tetO::his-3+, ridΔ, dim-5Δ, set-7Δ, mus-52Δ, mat a)
P2: C02.1 (ridΔ, his-3, mus-52Δ, mat A)
not sequenced
H
RIP propensity (%)
80
0
not sequenced
Wildtype
RID-deficient
500 bp
20
0
RIP propensity (%)

Figure 1